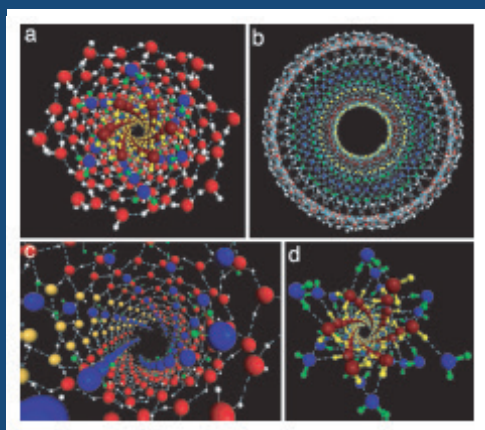


*Advances in Chemical Physics*  
Stuart A. Rice and Aaron R. Dinner, Series Editors

# Advances in Chemical Physics

Volume 156



Edited by  
Stuart A. Rice  
Aaron R. Dinner

WILEY



**ADVANCES IN CHEMICAL PHYSICS**

VOLUME 156

## EDITORIAL BOARD

KURT BINDER, Condensed Matter Theory Group, Institut Für Physik, Johannes Gutenberg-Universität, Mainz, Germany

WILLIAM T. COFFEY, Department of Electronic and Electrical Engineering, Printing House, Trinity College, Dublin, Ireland

KARL F. FREED, Department of Chemistry, James Franck Institute, University of Chicago, Chicago, Illinois USA

DAAN FRENKEL, Department of Chemistry, Trinity College, University of Cambridge, Cambridge, United Kingdom

PIERRE GASPARD, Center for Nonlinear Phenomena and Complex Systems, Université Libre de Bruxelles, Brussels, Belgium

MARTIN GRUBELE, Departments of Physics and Chemistry, Center for Biophysics and Computational Biology, University of Illinois at Urbana-Champaign, Urbana, Illinois USA

GERHARD HUMMER, Theoretical Biophysics Section, NIDDK-National Institutes of Health, Bethesda, Maryland USA

RONNIE KOSLOFF, Department of Physical Chemistry, Institute of Chemistry and Fritz Haber Center for Molecular Dynamics, The Hebrew University of Jerusalem, Israel

KA YEE LEE, Department of Chemistry, James Franck Institute, University of Chicago, Chicago, Illinois USA

TODD J. MARTINEZ, Department of Chemistry, Photon Science, Stanford University, Stanford, California USA

SHAUL MUKAMEL, Department of Chemistry, School of Physical Sciences, University of California, Irvine, California USA

JOSE N. ONUCHIC, Department of Physics, Center for Theoretical Biological Physics, Rice University, Houston, Texas USA

STEPHEN QUAKE, Department of Bioengineering, Stanford University, Palo Alto, California USA

MARK RATNER, Department of Chemistry, Northwestern University, Evanston, Illinois USA

DAVID REICHMAN, Department of Chemistry, Columbia University, New York City, New York USA

GEORGE SCHATZ, Department of Chemistry, Northwestern University, Evanston, Illinois USA

STEVEN J. SIBENER, Department of Chemistry, James Franck Institute, University of Chicago, Chicago, Illinois USA

ANDREI TOKMAKOFF, Department of Chemistry, James Franck Institute, University of Chicago, Chicago, Illinois USA

DONALD G. TRUHLAR, Department of Chemistry, University of Minnesota, Minneapolis, Minnesota USA

JOHN C. TULLY, Department of Chemistry, Yale University, New Haven, Connecticut, USA

# ADVANCES IN CHEMICAL PHYSICS

VOLUME 156

*Edited By*

**STUART A. RICE**

Department of Chemistry  
and  
The James Franck Institute,  
The University of Chicago,  
Chicago, Illinois

**AARON R. DINNER**

Department of Chemistry  
and  
The James Franck Institute,  
The University of Chicago,  
Chicago, Illinois

**WILEY**

Copyright © 2015 by John Wiley & Sons, Inc. All rights reserved.

Published by John Wiley & Sons, Inc., Hoboken, New Jersey.

Published simultaneously in Canada.

No part of this publication may be reproduced, stored in a retrieval system, or transmitted in any form or by any means, electronic, mechanical, photocopying, recording, scanning, or otherwise, except as permitted under Section 107 or 108 of the 1976 United States Copyright Act, without either the prior written permission of the Publisher, or authorization through payment of the appropriate per-copy fee to the Copyright Clearance Center, Inc., 222 Rosewood Drive, Danvers, MA 01923, (978) 750-8400, fax (978) 750-4470, or on the web at [www.copyright.com](http://www.copyright.com). Requests to the Publisher for permission should be addressed to the Permissions Department, John Wiley & Sons, Inc., 111 River Street, Hoboken, NJ 07030, (201) 748-6011, fax (201) 748-6008, or online at <http://www.wiley.com/go/permissions>.

**Limit of Liability/Disclaimer of Warranty:** While the publisher and author have used their best efforts in preparing this book, they make no representations or warranties with respect to the accuracy or completeness of the contents of this book and specifically disclaim any implied warranties of merchantability or fitness for a particular purpose. No warranty may be created or extended by sales representatives or written sales materials. The advice and strategies contained herein may not be suitable for your situation. You should consult with a professional where appropriate. Neither the publisher nor author shall be liable for any loss of profit or any other commercial damages, including but not limited to special, incidental, consequential, or other damages.

For general information on our other products and services or for technical support, please contact our Customer Care Department within the United States at (800) 762-2974, outside the United States at (317) 572-3993 or fax (317) 572-4002.

Wiley also publishes its books in a variety of electronic formats. Some content that appears in print may not be available in electronic formats. For more information about Wiley products, visit our web site at [www.wiley.com](http://www.wiley.com).

***Library of Congress Catalog Number: 58-9935***

ISBN: 978-1-118-94969-6

Printed in the United States of America

10 9 8 7 6 5 4 3 2 1

## CONTRIBUTORS TO VOLUME 156

ANASTASSIA N. ALEXandroVA, Department of Chemistry and Biochemistry, University of California, Los Angeles, CA, 90095-1569, USA

LOUIS-S. BOUCHARD, California NanoSystems Institute, Los Angeles, CA, 90095, USA

DECLAN J. BYRNE, School of Physics, University College Dublin, Belfield, Dublin 4, Ireland

WILLIAM T. COFFEY, Department of Electronic and Electrical Engineering, Trinity College, Dublin 2, Ireland

MARJOLEIN DIJKSTRA, Soft Condensed Matter group, Debye Institute for Nanomaterials Science, Utrecht University, Princetonplein 5, 3584 CC Utrecht, The Netherlands

WILLIAM J. DOWLING, Department of Electronic and Electrical Engineering, Trinity College, Dublin 2, Ireland

M. HAYASHI, Condensed Matter Center, National Taiwan University, Taipei, Taiwan

YURI P. KALMYKOV, Laboratoire de Mathématiques et Physique, Université de Perpignan Via Domitia, 54, Avenue Paul Alduy, F-66860 Perpignan, France

C.K. LIN, Condensed Matter Center, National Taiwan University, Taipei, Taiwan

S.H. LIN, Department of Applied Chemistry, National Chiao-Tung University, Hsinchu, Taiwan

G. ALI MANSOORI, Department of Bioengineering, University of Illinois at Chicago, Chicago, IL 60607-7052, USA

Y.L. NIU, The State Key Laboratory of Molecular Reaction Dynamics, Institute of Chemistry, Chinese Academy of Sciences, Beijing, China

RANKO RICHERT, Department of Chemistry and Biochemistry, Arizona State University, Tempe, AZ, 85287-1604, USA

STUART A. RICE, Department of Chemistry and the James Franck Institute, The University of Chicago, Chicago, IL 60637, USA

ASAF SHIMSHOVITZ, Department of Chemical Physics, Weizmann Institute of Science, Rehovot, 76100 Israel

NORIO TAKEMOTO, Department of Chemical Physics, Weizmann Institute of Science, Rehovot, 76100 Israel

DAVID J. TANNOR, Department of Chemical Physics, Weizmann Institute of Science, Rehovot, 76100 Israel

SERGUEY V. TITOV, Kotel'nikov Institute of Radio Engineering and Electronics of the Russian Academy of Sciences, Vvedenskii Square 1, Fryazino, Moscow Region, 141190, Russian Federation

L. YANG, Institute of Theoretical and Simulation Chemistry, Academy of Fundamental and Interdisciplinary Science, Harbin Institute of Technology, Harbin, China

C.Y. ZHU, Department of Applied Chemistry, National Chiao-Tung University, Hsinchu, Taiwan

## PREFACE TO THE SERIES

Advances in science often involve initial development of individual specialized fields of study within traditional disciplines followed by broadening and overlap, or even merging, of those specialized fields, leading to a blurring of the lines between traditional disciplines. The pace of that blurring has accelerated in the last few decades, and much of the important and exciting research carried out today seeks to synthesize elements from different fields of knowledge. Examples of such research areas include biophysics and studies of nanostructured materials. As the study of the forces that govern the structure and dynamics of molecular systems, chemical physics encompasses these and many other emerging research directions. Unfortunately, the flood of scientific literature has been accompanied by losses in the shared vocabulary and approaches of the traditional disciplines, and there is much pressure from scientific journals to be ever more concise in the descriptions of studies, to the point that much valuable experience, if recorded at all, is hidden in supplements and dissipated with time. These trends in science and publishing make this series, *Advances in Chemical Physics*, a much needed resource.

The *Advances in Chemical Physics* is devoted to helping the reader obtain general information about a wide variety of topics in chemical physics, a field that we interpret very broadly. Our intent is to have experts present comprehensive analyses of subjects of interest and to encourage the expression of individual points of view. We hope that this approach to the presentation of an overview of a subject will both stimulate new research and serve as a personalized learning text for beginners in a field.

STUART A. RICE  
AARON R. DINNER



# CONTENTS

PHASE SPACE APPROACH TO SOLVING THE SCHRÖDINGER EQUATION: THINKING INSIDE THE BOX	1
<i>David J. Tannor, Norio Takemoto, and Asaf Shimshovitz</i>	
ENTROPY-DRIVEN PHASE TRANSITIONS IN COLLOIDS: FROM SPHERES TO ANISOTROPIC PARTICLES	35
<i>Marjolein Dijkstra</i>	
SUB-NANO CLUSTERS: THE LAST FRONTIER OF INORGANIC CHEMISTRY	73
<i>Anastassia N. Alexandrova and Louis-S. Bouchard</i>	
SUPERCOOLED LIQUIDS AND GLASSES BY DIELECTRIC RELAXATION SPECTROSCOPY	101
<i>Ranko Richert</i>	
CONFINED FLUIDS: STRUCTURE, PROPERTIES AND PHASE BEHAVIOR	197
<i>G. Ali Mansoori and Stuart A. Rice</i>	
THEORIES AND QUANTUM CHEMICAL CALCULATIONS OF LINEAR AND SUM-FREQUENCY GENERATION SPECTROSCOPIES, AND INTRAMOLECULAR VIBRATIONAL REDISTRIBUTION AND DENSITY MATRIX TREATMENT OF ULTRAFAST DYNAMICS	295
<i>L. Yang, Y.L. Niu, C.K. Lin, M. Hayashi, C.Y. Zhu, and S.H. Lin</i>	
ON THE KRAMERS VERY LOW DAMPING ESCAPE RATE FOR POINT PARTICLES AND CLASSICAL SPINS	393
<i>Declan J. Byrne, William T. Coffey, William J. Dowling, Yuri P. Kalmykov, and Serguey V. Titov</i>	
AUTHOR INDEX	461
SUBJECT INDEX	499



# PHASE SPACE APPROACH TO SOLVING THE SCHRÖDINGER EQUATION: THINKING INSIDE THE BOX

DAVID J. TANNOR, NORIO TAKEMOTO, and ASAF SHIMSHOVITZ

*Department of Chemical Physics, Weizmann Institute of Science, Rehovot,  
76100 Israel*

## CONTENTS

- I. Introduction
- II. Theory
  - A. von Neumann Basis on the Infinite Lattice
  - B. Fourier Method
  - C. The Periodic von Neumann Basis (pvN)
  - D. Biorthogonal von Neumann Basis Set (bvN)
  - E. Periodic von Neumann Basis with Biorthogonal Exchange (pvb)
- III. Application to Ultrafast Pulses
- IV. Applications to Quantum Mechanics
  - A. Time-independent Schrödinger Equation (TISE)
    - 1. Formalism
    - 2. 1D Applications
    - 3. Multidimensional Applications
    - 4. Scaling of the Method with  $\hbar$  and with Dimensionality
    - 5. Wavelet Generalization
  - B. Time-dependent Schrödinger Equation (TDSE)
- V. Applications to Audio and Image Processing
- VI. Conclusions and Future Prospects
- Acknowledgments
- References

## I. INTRODUCTION

In 1946, Gabor proposed using a set of Gaussians located on a time–frequency lattice as a basis for representing arbitrary signals [1]. Gabor’s motivation can be understood by considering Fig. 1a. If one considers an acoustical signal, generally

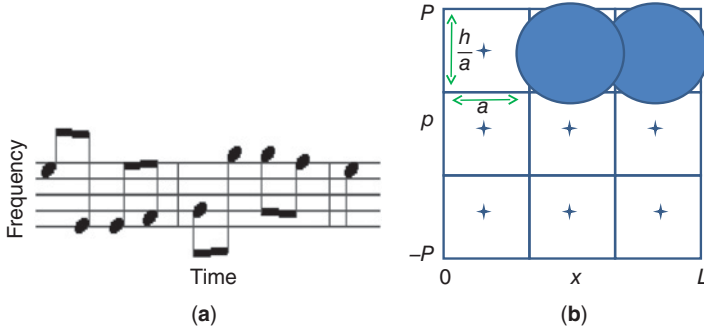


**Figure 1.** (a) A section of Beethoven’s fifth symphony, showing that if a musical score is viewed as a plot of the time–frequency plane there is strong correlation between frequency and time. Note that most of the time–frequency phase space cells are empty. (b) A schematic representation of the von Neumann lattice in which one Gaussian is placed in every phase space cell of area  $h$ . For a color version of this figure, see the color plate section.

there is some form of time–frequency correlation. This is made explicit in musical notation, where the score can be thought of as a two-dimensional (2D) time–frequency plot, showing schematically that not all frequencies are present at all times. Gabor’s proposal was to divide this 2D time–frequency space into cells of area  $2\pi$  and place one Gaussian per cell. If the Gaussians are considered as a basis set, intuitively a substantial fraction of the Gaussians may be expected to have near-vanishing coefficients.

It turns out that the identical lattice of Gaussians was discovered by von Neumann 15 years earlier in the context of quantum mechanics, where instead of  $\omega$  and  $t$  the conjugate variables are  $p$  and  $x$  and the area of the unit cell is  $h$  [2]. However, in all respects the formalism is isomorphic. Von Neumann’s interest was in a generalized uncertainty principle, but subsequently mathematical physicists explored the properties of the von Neumann lattice as a basis. It was proven that if one Gaussian is placed per cell of area  $h$  the von Neumann basis is complete but not overcomplete, provided the width parameter of the Gaussian is appropriate to the cell size [3]. In the late 1970s, Davis and Heller [4] explored the use of the vN basis for solving the time-independent Schrödinger equation (TISE). Their motivation was similar to that of Gabor’s. They reasoned that the classical mechanical phase space contour at energy  $E$  should provide an excellent guide for where quantum mechanical basis functions are needed. To the extent that basis functions outside the classical contour can be eliminated, the basis should provide a very efficient representation. Some prototypical examples of classical energy contours are illustrated in Fig. 2.

Although the commercial aspects of the representation are probably much larger for audio and image processing than for quantum mechanics, the advantage of the von Neumann representation is potentially much higher in quantum

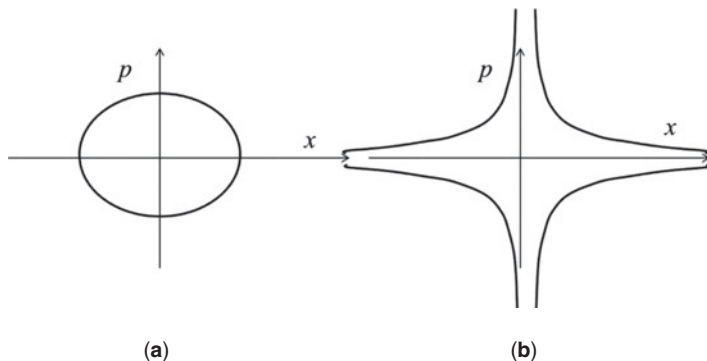


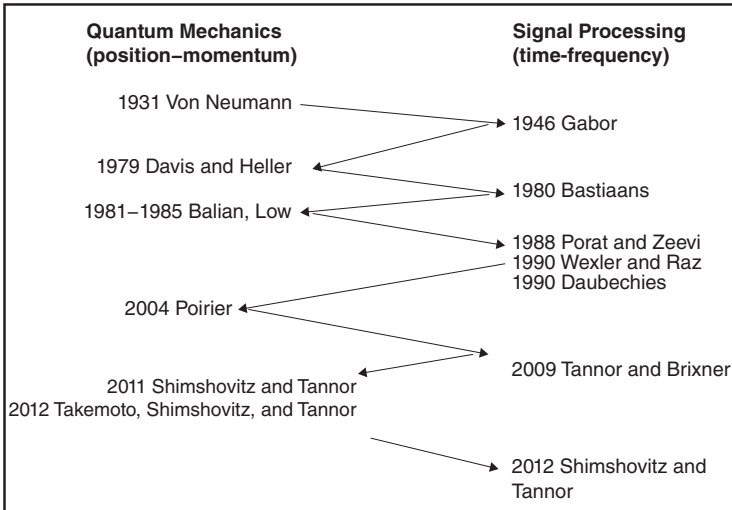
**Figure 2.** Classical phase space contours for (a) harmonic oscillator Hamiltonian, (b) Coulomb Hamiltonian.

mechanics. The reason is that quantum mechanical calculations for realistic atoms and molecules involve solving a wave equation in  $3N$  degrees of freedom, where  $N$  is the number of electrons and nuclei, a dimensionality much higher than one deals with in signal and image processing. Most basis function methods use a tensor product Hilbert space and as a result the number of basis functions grows exponentially with the number of degrees of freedom. This notorious problem is called the “exponential wall” [5]. Although the von Neumann basis functions in multidimensions are direct products of one-dimensional (1D) Gaussians, the Hilbert space after removing the energetically inaccessible Gaussians is *not* a tensor product Hilbert space. Thus, formally at least, the method has the potential to defeat the exponential wall in basis set calculations.

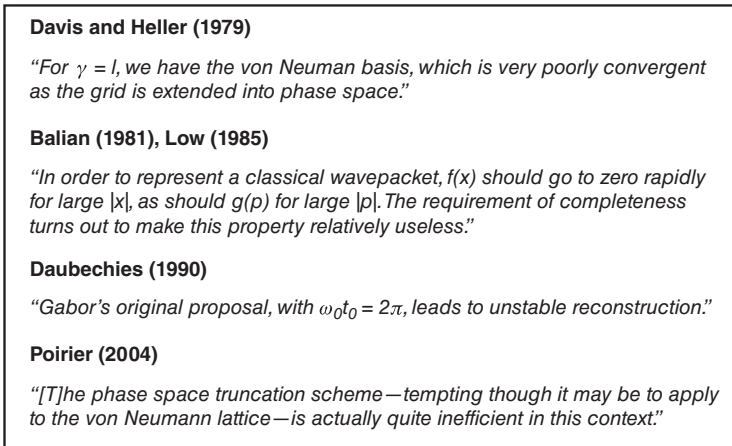
Due to its intuitive appeal and its potential for simple and efficient representation, the von Neumann representation has attracted interest in the theoretical chemistry community since the late 1970s. Similarly, the Gabor representation has attracted interest in the signal processing community since its invention in 1946, with a peak of interest in the 1980s and 1990s. The development of the theory in these two fields has been nearly independent, with only limited transfer of ideas and methods between these communities. Figure 3a summarizes some of the key milestones in the development of von Neumann/Gabor theory [1, 2, 4, 6–19].

One of the striking parallels in the development of the method in quantum mechanics and signal processing is that the method never became mainstream in either community. A key reason is undoubtedly the problems encountered in converging the method, problems reported independently in both fields. Figure 3b collects some quotations from the literature, both in quantum mechanics and in signal processing, that testify to the problems with convergence of the method [4, 7, 8, 11, 12].

We have recently discovered a simple but surprising way to converge the von Neumann/Gabor method [15–19]. Our insight was to define a modified



(a)



(b)

**Figure 3.** (a) A schematic diagram of the development of the von Neumann/Gabor method in the quantum mechanics and signal processing communities. The development proceeded largely independently. (b) Quotes from the quantum mechanics and signal processing literatures indicating that the von Neumann/Gabor basis on a truncated lattice does not converge.

von Neumann/Gabor basis in which the boundary conditions are taken to be periodic and band limited. As we show below, this ensures that the representation has exact informational equivalence with the Fast Fourier Transform method, which has been used so profitably for quantum dynamics calculations. In the language of signal processing, the significance of this result is that the modified Gabor basis

satisfies a Nyquist–Shannon sampling theorem [20–22], meaning that the representation is exact for functions that are band limited and periodic, and converges exponentially fast for functions that decay exponentially in both time and frequency. The net result is that the periodic von Neumann (pvN) or periodic Gabor (pg) basis combines the best of both worlds: Gaussian flexibility with Fourier accuracy.

One more development is crucial to making the method useful. Although the periodic von Neumann representation has complete informational equivalence with the Fourier representation if the full basis is kept, it turns out that discarding even a single pvN function incurs a considerable error—actually a much larger error than incurred in discarding Fourier functions. In other words, Gabor’s original proposal for compression turns out not only to fail, but to have exactly the opposite consequences of what he expected. To understand the problem and its solution, note that the von Neumann basis is non-orthogonal. As a result, the basis functions do not satisfy a Kronecker delta relation  $\langle g_m | g_n \rangle = \delta_{mn}$ , but rather a relation  $\langle b_m | g_n \rangle = \delta_{mn}$  where the  $\{b_m\}$  are a set of basis functions biorthogonal to the  $\{g_n\}$ . Although the  $\{g_n\}$  are localized the  $\{b_m\}$  are not. In the implementation of the vN representation as envisioned by Gabor and all subsequent work, the  $\{g_n\}$  are the basis functions and therefore the delocalized  $\{b_m\}$  determine the coefficients. Our finding was that by interchanging the role of the basis and its biorthogonal basis we obtain a delocalized basis  $\{b_m\}$  but the localized functions  $\{g_n\}$  now determine the coefficients, many of which are now nearly vanishing.

The remainder of this review is organized as follows. Section II presents the basic theory. Sections III–V present applications, first to femtosecond pulse shaping, then to quantum mechanics (both time independent and time dependent) and finally to audio and image processing. Section VI is a Conclusion with some discussion of future directions.

## II. THEORY

### A. von Neumann Basis on the Infinite Lattice

The von Neumann basis set [2] is a subset of the “coherent states” of the form:

$$g_{nl}(x) = \left(\frac{2\alpha}{\pi}\right)^{\frac{1}{4}} \exp\left(-\alpha(x - x_n)^2 + i\frac{p_l}{\hbar}(x - x_n)\right) \quad (1)$$

where  $n$  and  $l$  are integers. Each basis function is a Gaussian centered at  $(x_n, p_l) = (na + x_0, \frac{\hbar}{a} + p_0)$  in phase space, where  $x_0$  and  $p_0$  are arbitrary shifts. The parameter  $\alpha = \frac{\sigma_p}{2\sigma_x}$  controls the FWHM of each Gaussian in  $x$  and  $p$  space. Taking  $\Delta x = a$ ,  $\Delta p = \hbar/a$  as the spacing between neighboring Gaussians in  $x$  and  $p$  space respectively, we note that  $\Delta x \Delta p = \hbar$  so we have exactly one basis function per unit cell in phase space. As shown in [3] this implies completeness in the Hilbert space.

The “complete” vN basis, where  $n$  and  $l$  run over all integers, spans the infinite Hilbert space. In any numerical calculation, however,  $n$  and  $l$  take on a finite number of values, producing  $N$  Gaussian basis functions  $\{g_i(x)\}$ ,  $i = 1 \dots N$ . Since the size of one vN unit cell is  $h$ , the area of the truncated vN lattice is given by  $S^{\text{vN}} = Nh$ .

## B. Fourier Method

Before proceeding to describe our modified version of the von Neumann lattice, we need to present some background about the Fourier method.

The pseudospectral Fourier method [23, 24] (also known as the sinc discrete variable representation (DVR) [25]) is a widely used tool in quantum simulations [26–29]. In this method a function  $\psi(x)$  that is periodic in  $L$  and band limited in  $K = \frac{P}{\hbar}$  can be written in the following form:  $\psi(x) = \sum_{n=1}^N \psi(x_n)\theta_n(x)$ , where  $x_n = \delta_x(n - 1)$ , and  $\delta_x = \frac{\pi\hbar}{P} = \frac{L}{N}$ . The basis functions  $\{\theta_n(x)\}$  are given by [30]:

$$\theta_n(x) = \sum_{j=-\frac{N}{2}+1}^{\frac{N}{2}} \frac{1}{\sqrt{LN}} \exp\left(\frac{i2\pi j}{L}(x - x_n)\right), \quad (2)$$

which can be shown to be sinc functions that are periodic on the domain  $[0, L]$  [31]. A couple of representative functions from this set are illustrated in Fig. 4.

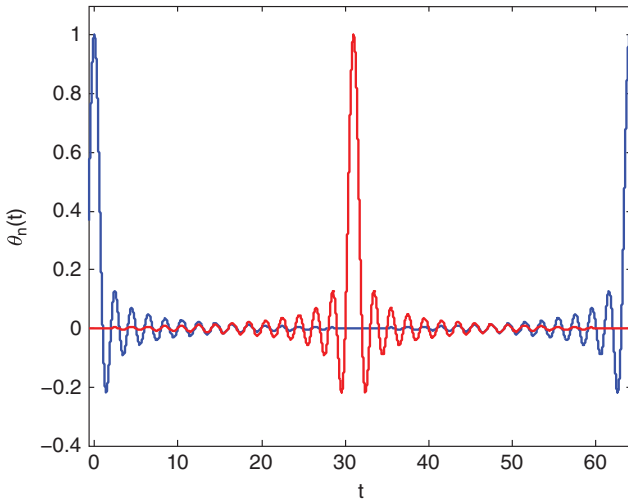


**Figure 4.** Illustration of the Dirichlet or periodic sinc functions. These functions are the underlying basis of the fast Fourier transform (discrete Fourier transform with periodic boundary conditions). They go to 1 at one of the Fourier grid points and to 0 at all the other Fourier grid points. The various members of the basis are orthonormal. For a color version of this figure, see the color plate section.

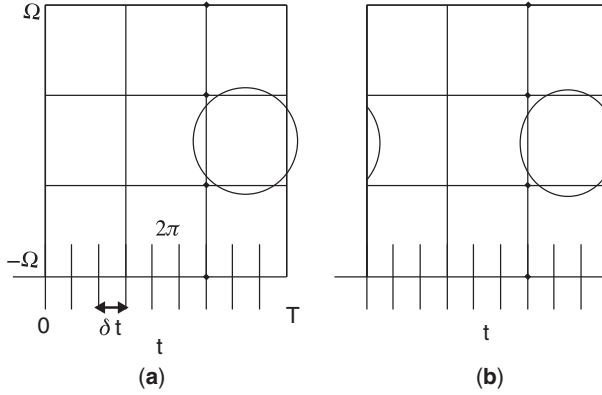


**Figure 5.** (a)  $N = 9$  coordinate grid points and  $N = 9$  Gabor unit cells cover the same area in phase space,  $S = 2\pi N$ . Superimposed is a typical Gabor function. Note that its boundary conditions are not appropriate for the rectangular area. (b) The periodic Gabor (pg) basis is a complete set for the truncated space. The pg basis functions are, loosely speaking, periodic and band-limited Gaussians whose centers are located at the center of each unit cell.

By Nyquist's theorem, if the spacing between points in the Fourier method is  $\delta x$ , the frequency range that can be spanned is  $2P = 2\frac{\pi\hbar}{\delta x}$ . Thus, the set  $\{\theta_i(x)\}$   $i = 1, \dots, N$  spans a rectangular shape in phase space with area  $S^{\text{FGH}} = 2LP = 2L\frac{\pi\hbar}{\delta x} = Nh$  [23]. Thus  $N$  unit cells in the vN lattice and  $N$  grid points in the Fourier method cover the same rectangle with an area in phase space of (Fig. 5a):

$$S^{\text{vN}} = S^{\text{FGH}} = Nh. \quad (3)$$

This suggests that  $N$  vN basis functions confined to this area will be equivalent to the Fourier basis set. Unfortunately, the attempt to use  $N$  Gaussians as a basis set for this phase space area leads to extremely large numerical errors. One may think of this as a result of Gaussians on the edges of Fig. 5a protruding from the truncated space; as a consequence, there are also gaps in the coverage of the Hilbert space of the interior region.

### C. The Periodic von Neumann Basis (pvN)

The problem with convergence of the truncated lattice of Gaussians can be overcome by combining the Gaussian and the Fourier basis functions, generating a "Gaussian-like" basis set that completely spans the truncated space. Specifically,

the  $\{g_m(x)\}$  functions enter as the coefficients of the Dirichlet functions  $\{\theta_i(x)\}$  to construct a new basis set,  $\{\tilde{g}_m(x)\}$ :

$$\tilde{g}_m(x) = \sum_{n=1}^N \theta_n(x) g_m(x_n) \quad (4)$$

for  $m = 1, \dots, N$ . The new basis set is in some sense, the Gaussian functions with periodic boundary conditions and band limited, henceforth the periodic von Neumann or pvN basis (Fig. 5b). We can write Eq. (4) in matrix notation as:  $\tilde{\mathbf{G}} = \Theta \mathbf{G}$ , where  $G_{ij} = g_j(x_i)$ . By taking the width parameter  $\alpha = \frac{\Delta p}{2h\Delta x}$  we guarantee that the pvN functions have no linear dependence and that the matrix  $\mathbf{G}$  is invertible, that is  $\tilde{\mathbf{G}}\mathbf{G}^{-1} = \Theta$ . The invertibility of  $\mathbf{G}$  implies that the  $\{\tilde{g}_m(x)\}$  and the  $\{\theta_i(x)\}$  span the same Hilbert space and therefore are informationally equivalent representations.

Inspection of Fig. 5b explains why the subtitle of this review is “thinking inside the box.”

#### D. Biorthogonal von Neumann Basis Set (bvN)

Although the pvN and the Fourier methods span the same rectangle in phase space, in the Fourier basis one is constrained to a rectangular area in phase space whereas in the pvN method one has the freedom to place basis functions only where needed in phase space. If the classical phase space up to energy  $E$  occupies only a small fraction of the circumscribed rectangular area, the pvN basis can lead to significant savings. This is particularly important for multidimensional problems, where the savings in the pvN actually grows faster than exponentially with dimension, as discussed in Section II E. below. However, there is an important subtlety in discarding basis functions that arises because the basis is non-orthogonal. We therefore provide a brief review of some properties of non-orthogonal bases.

For an orthonormal basis, we have the relation:

$$\langle \phi_m | \phi_n \rangle = \delta_{mn}. \quad (5)$$

For a non-orthogonal basis this relation does not in general hold and one writes:

$$\langle g_m | g_n \rangle = S_{mn}, \quad (6)$$

where  $\mathbf{S}$  is the overlap matrix. Alternatively, one can write:

$$\langle b_m | g_n \rangle = \langle g_m | b_n \rangle = \delta_{mn} \quad (7)$$

where the set  $\{b_m\}$  is called the basis “biorthogonal” to the set  $\{g_n\}$ . The usual completeness relation for orthogonal bases:

$$\sum_{n=1}^{\infty} |\phi_n\rangle\langle\phi_n| = \mathbf{1} \quad (8)$$

is replaced by the relations:

$$\sum_{n=1}^{\infty} |g_n\rangle\langle b_n| = \sum_{n=1}^{\infty} |b_n\rangle\langle g_n| = \mathbf{1}. \quad (9)$$

To obtain an explicit relation for the  $\{b_n\}$  we note the following alternative expression for the completeness relation for a non-orthogonal basis [32]:

$$\sum_{n=1}^{\infty} \sum_{m=1}^{\infty} |g_m\rangle(S^{-1})_{mn}\langle g_n| = \mathbf{1}. \quad (10)$$

Comparing Eq. (10) with Eq. (9) we see that

$$|b_n\rangle = \sum_{m=1}^{\infty} |g_m\rangle(S^{-1})_{mn}, \quad (11)$$

or on the truncated space

$$|\tilde{b}_n\rangle = \sum_{m=1}^N |\tilde{g}_m\rangle(S^{-1})_{mn}. \quad (12)$$

Figure 6 shows a plot of the  $\mathbf{S}$  and the  $\mathbf{S}^{-1}$  matrices on a logarithmic scale. As seen clearly in the figure, although the  $\mathbf{S}$  matrix is tightly banded, the  $\mathbf{S}^{-1}$  decays slowly away from the diagonal. As a consequence, although the  $\{g_i\}$  basis is localized, the  $\{b_i\}$  basis is delocalized. Figure 7 shows a typical  $b_n$  basis function, which is seen to be not only delocalized but to be quite irregularly shaped with discontinuous derivatives.

### E. Periodic von Neumann Basis with Biorthogonal Exchange (pvb)

We now return to the issue of discarding unnecessary basis functions. If  $|\psi\rangle$  occupies only a fraction of the rectangle spanned by the Fourier basis, we may expect that many of the pvN basis functions will fulfill the relation:  $\langle\tilde{g}_j|\psi\rangle = 0$ ,  $j = 1, \dots, M$ . However, due to the non-orthogonality of the basis we cannot simply

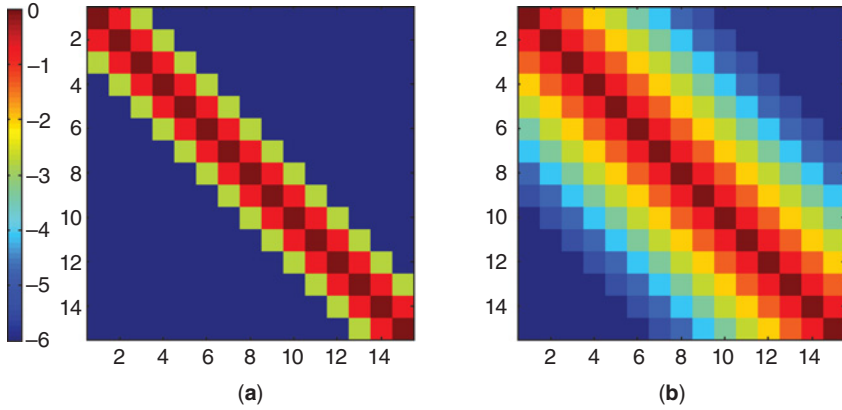


**Figure 6.** Magnitude of  $\mathbf{S}$  (a) and  $\mathbf{S}^{-1}$  (b) matrices on a logarithmic scale. For a color version of this figure, see the color plate section.

eliminate the states  $\tilde{g}_j$ , since the *coefficients* of  $\tilde{g}_j$  are not simply given by  $\langle \tilde{g}_j | \psi \rangle = 0$ . To see this, consider the representation of the state  $|\psi\rangle$  in the pvN basis set:

$$|\psi\rangle = \sum_{m=1}^N |\tilde{g}_m\rangle a_m = \sum_{n=1}^N \sum_{m=1}^N |\tilde{g}_m\rangle (S^{-1})_{mn} \langle \tilde{g}_n | \psi \rangle, \quad (13)$$

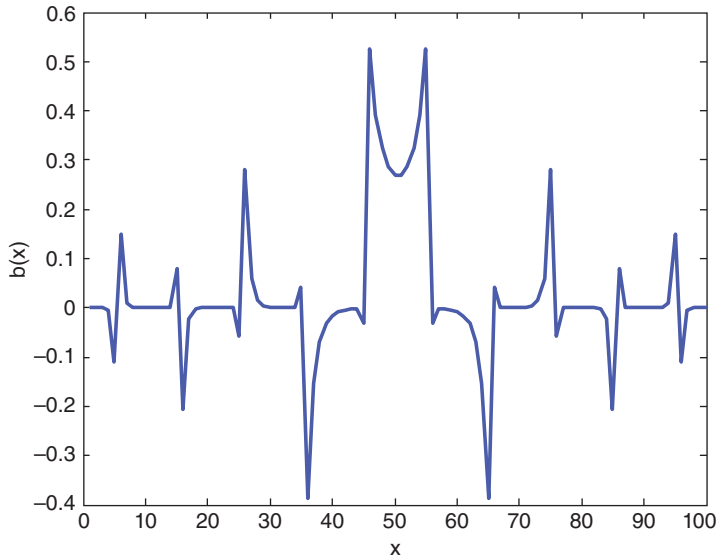


**Figure 7.** A typical biorthogonal basis function.

where in the second equality we have used the completeness relationship for non-orthogonal bases, Eq. (10), applied to the truncated space. Comparing the two expressions in Eq. (13) we find that

$$a_m = \sum_{n=1}^N (S^{-1})_{mn} \langle \tilde{g}_n | \psi \rangle. \quad (14)$$

The expression for the coefficients  $a_m$  is seen to contain  $\mathbf{S}^{-1}$ . Since as discussed above  $\mathbf{S}^{-1}$  is delocalized,  $a_m$  can be quite significant, even if  $g_m$  is remote from  $\psi$  because  $a_m$  can draw amplitude from non-remote  $\langle \tilde{g}_n | \psi \rangle$ . Nevertheless, we can still take advantage of the many near-vanishing  $\langle \tilde{g}_n | \psi \rangle$  to obtain a compact representation of the function  $|\psi\rangle$ . The key is to exchange the role of the  $\{g_n\}$  and  $\{b_m\}$  basis sets. Substituting Eq. (12) into Eq. (13),  $|\psi\rangle$  can be written as

$$|\psi\rangle = \sum_{n=1}^N |\tilde{b}_n\rangle c_n = \sum_{n=1}^N |\tilde{b}_n\rangle \langle \tilde{g}_n | \psi \rangle. \quad (15)$$

By assumption,  $M$  of the coefficients are zero, hence only  $N' = N - M$  basis functions are necessary in order to represent  $|\psi\rangle$  in this basis. Note that the new basis functions, the  $\{b_n\}$ , are not only delocalized but have discontinuous derivatives (see Fig. 7); paradoxically, this is the farthest thing from the localized basis envisioned by Gabor and by his counterparts in the quantum community! However, this highly irregular basis is exactly what is needed to ensure that the localized functions  $\{g_n\}$  determine the coefficients, and hence that the representation is as sparse as possible.

The equations take a particularly compact form in matrix notation: Eq. (12) becomes  $\mathbf{B} = \mathbf{G}\mathbf{S}^{-1} = (\mathbf{G}^\dagger)^{-1}$  or  $\mathbf{G}^\dagger\mathbf{B} = \mathbf{1}$  at the Fourier grid points.

The biorthogonal basis is well known in the signal processing literature [6, 9, 10, 33–35], but the crucial idea of exchanging the roles of the pvN and the bvN seems to have been overlooked. We attribute this to the fact that Eq. (10) involving  $\mathbf{S}^{-1}$  does not appear in that literature. It is this expression, together with the non-sparseness of the  $\mathbf{S}^{-1}$  matrix that provides the motivation for the exchange of roles. To distinguish our method from previous work we call our method the “periodic von Neumann with biorthogonal exchange” method or pvb. When applying the method to signal processing we refer to it as the “periodic Gabor with biorthogonal exchange” method or pgb.

### III. APPLICATION TO ULTRAFAST PULSES

As a first illustration of the use of the periodic Gabor basis we consider the representation of shaped femtosecond laser pulses that emerge in the field of quantum

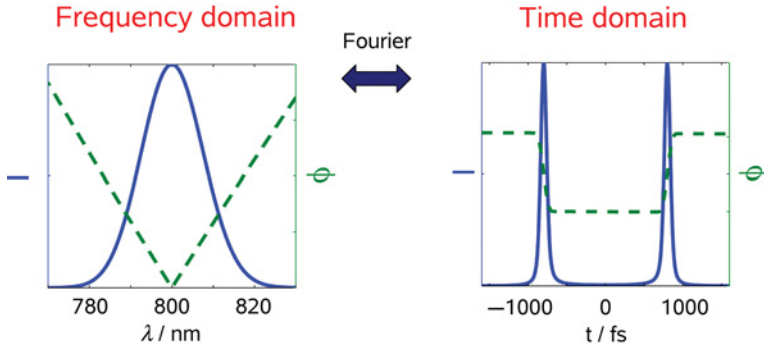


**Figure 8.** Example of a non-intuitive Fourier transform pair. The solid line shows the amplitude and the dashed line the phase. The “V” phase profile in frequency leads to a double-pulse structure in time.

control [36–41]. These pulses are complex, and in general are shaped in both amplitude and phase. We start with this example for three reasons. First, chronologically this was our first application of the von Neumann lattice [14, 15]. Second, it provides a nice comparison of the visual form of the discrete Gabor representation with the Wigner and Husimi representations. Third, it shows the importance of the periodic boundary conditions in the Gabor representation without the additional complications of quantum mechanical operators. In Section IV, when we turn to the quantum mechanical applications, all the considerations introduced in this section will still apply, with additional methods required to represent operators in the pvb basis.

Figure 8 shows a shaped laser pulse in both the frequency and time representations. In frequency, it consists of a Gaussian amplitude multiplied by a “V” phase profile. In the time domain, related by a Fourier transform, the “V” phase profile leads to a double-pulse structure. Although both the frequency and time representations contain the same information, it is difficult to appreciate all the properties of the signal from one representation alone.

Figure 9a shows the same signal in the Wigner representation [42]. The marginals of the Wigner representation give the absolute value squared in the frequency and time representations, respectively. However, in the Wigner representation one can visualize simultaneously both the single-lobed structure of the frequency profile and the double-lobed structure of the time profile. Note that the Wigner representation shows oscillations between the two portions of the pulse in time. These oscillations can take on negative values, making it impossible to interpret the Wigner representation strictly as a probability distribution. Figure 9b shows the Husimi representation of the same signal. The Husimi representation is defined as the absolute value squared of the overlaps of the signal with a continuous-parameter set of time–frequency Gaussians [43], and therefore unlike

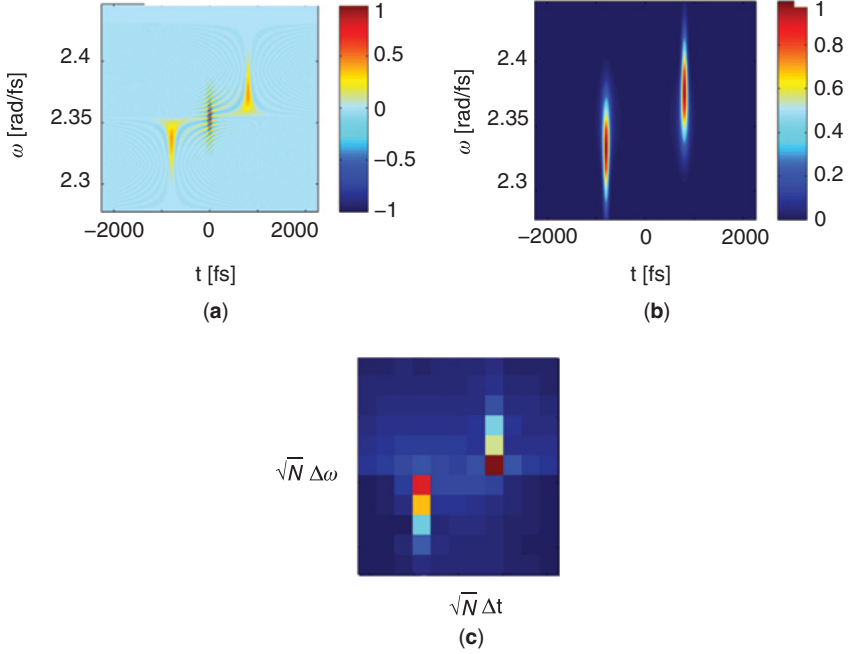


**Figure 9.** The Wigner representation (a), the Husimi representation (b), and the von Neumann representation (c) of the pulse in Fig. 8. All three representations allow the visualization of the pulse in time and frequency simultaneously. For a color version of this figure, see the color plate section.

the Wigner representation is everywhere positive semidefinite. Formally, one can show that the Husimi representation is a Gaussian smoothing of the Wigner representation, and in fact one can see that the oscillations in the Wigner representation are washed out in the Husimi representation.

Figure 9c shows the signal of Fig. 8 in the von Neumann/Gabor representation. Since the basis set is discrete so is the representation. The major features of the signal in both frequency and time are clearly observed. The discreteness of the representation, which at first sight may appear somewhat jarring, is actually its strength, providing exactly the same number of parameters as the discrete Fourier representation.

As a first test of the von Neumann representation, in Fig. 10 we consider whether the transformation of a signal to the von Neumann representation is invertible. The red curve in Fig. 10c portrays the amplitude profile of a frequency signal defined at a finite, discrete number of points. Such a discrete representation occurs naturally when considering shaped ultrafast pulses, since the masks used for pulse shaping consist of a finite, discrete number of pixels. Figure 10a–b show the amplitude and phase respectively of the von Neumann representation. The back-transformed signal is shown as the blue curve in Fig. 10c, and differs significantly from the

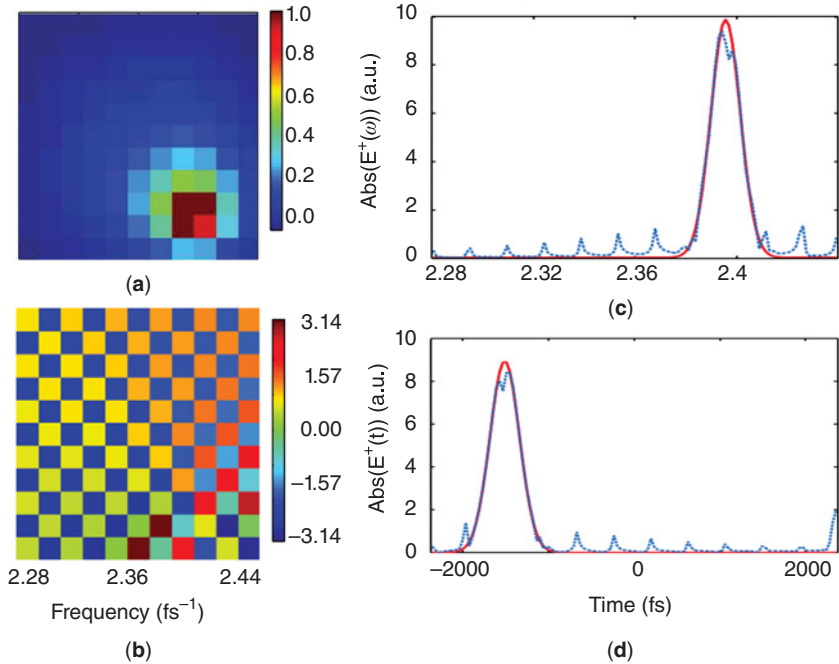


**Figure 10.** Transformation of a Gaussian pulse from frequency to the von Neumann representation and back without periodic boundary conditions. The error in the back-transformed signal is quite significant (blue vs. red curve in (c)). Panel (a) shows the amplitude of the von Neumann representation and panel (b) the phase. Adapted from Ref. [15]. For a color version of this figure, see the color plate section.

original signal. However, when the conventional von Neumann basis is replaced by the pvN basis, the representation in Fig. 11a–b is obtained. The periodic boundary conditions are clearly visible in the figure, with the effect that the ringing in the interior region that is present Fig. 10a is eliminated. When Fig. 11a is back-transformed to frequency, the signal is indistinguishable from the original (red curve in Fig. 11c), and in fact the two signals are identical to the precision of the computer. This shows the dramatic effect of the periodic boundary conditions on the von Neumann representation.

#### IV. APPLICATIONS TO QUANTUM MECHANICS

We now turn to the main topic of this review, the application of the pvb method to quantum mechanics. In this section we discuss the application to the TISE and in the next section we will discuss the application to the time-dependent Schrödinger equation.

- multiple aromaticity and
  - antiaromaticity, 75–80, 95
  - super-atom model, 86–88
- overview, 73–75
- technologies and opportunities, 88–95
  - cluster motors, 90–92
  - clusters in catalysis, 92–95
  - new inorganic ligands and building blocks, 88
  - superconductivity in metal clusters, 88–90
- Sum-frequency generation (SFG)
  - spectroscopy, 296
  - applications of, 335–341
    - to biosciences, 339–341
    - to dye-sensitized solar cells, 338–339
    - to water interface, 335–338
  - double resonance
    - energy level diagram for, 325, 329
    - for Rhodmin 6G, 326–327, 328
  - of ethylbenzene–and styrene–oligomer–graphene systems, 325
  - phase effect on, 323
  - resonance–off-resonance, energy level diagram for, 321
  - stochastic Liouville equation, 317
  - theory of, 317–335
    - electronic sum-frequency generation, 327–334
    - susceptibility method, 317–321
    - vibrational sum-frequency generation, 321–327
- Super-atom model, and sub-nano inorganic clusters, 86–88
- Superballs, phase diagrams of, 60–61
- Superconductivity, in metal clusters, 88–90
- Supercooled liquids and glasses, and dielectric relaxation spectroscopy, 102–184
  - applications, 152–183
    - conductivity, 168–170
    - dynamic equilibrium properties, 155–164
    - dynamic nonequilibrium properties, 164–168
    - heterogeneous dielectrics/ confinement, 173–176
    - local detection, 170–173
    - nonlinear experiments, 176–183
    - relation to other variables, 183
    - static properties, 152–155
  - linear experimental techniques, 134–147
    - capacitors for permittivity measurements, 141–144
    - frequency-domain methods, 138–140
    - limitations from blocking electrodes, 144–147
    - noise measurements, 140–141
    - thermally stimulated depolarization, 136–138
    - time-domain methods, 134–136
  - nonlinear experimental techniques, 147–152
    - large AC fields, 148–150
    - large DC fields, 147–148
    - pump-probe techniques, 150–152
- overview, 102–104
- permittivity fundamentals, 104–118
  - fluctuations and noise, 115–118
  - frequency-domain relations, 112–115
  - steady state equations, 104–109
  - time-domain relations, 109–112
- response functions, 118–133
  - conductivity, 132–133
  - Debye response, 118–122
  - dispersive, 123–132

- Superposition approach, and  
dielectric relaxation  
spectroscopy, 123–124
- Susceptibility method, SFG  
spectroscopy, 317–321  
dipole approximation, 318  
Liouville operators, 317  
second-order nonlinear  
susceptibility, 319–320  
second-order polarization, 318  
stochastic Liouville equation, 317
- TDDFT, *see* Time-dependent DFT  
(TDDFT)
- TDR, *see* Time-domain reflection  
(TDR)
- TDSE, *see* Time-dependent  
Schrödinger Equation (TDSE)
- Technologies and opportunities,  
cluster-based, 88–95  
cluster motors, 90–92  
clusters in catalysis, 92–95  
new inorganic ligands and building  
blocks, 88  
superconductivity in metal clusters,  
88–90
- Time-dependent DFT (TD-DFT),  
31–32, 312
- Time-dependent Schrödinger  
Equation (TDSE), 23–28
- Time-domain functions, and dielectric  
experiments  
dispersive response functions,  
124–125  
linear experimental techniques,  
134–136  
permittivity fundamentals, 109–112
- Time-domain reflection (TDR), 135
- Time-independent Schrödinger  
Equation (TISE), 15–23  
formalism, 15–18  
multidimensional applications,  
18–20  
scaling of method with  $h$  and with  
dimensionality, 20–21  
wavelet generalization, 21–23
- Time-resolved photodissociation  
(TRPD), 341
- Time-temperature superposition  
(TTS), 161
- TISE, *see* Time-independent  
Schrödinger Equation (TISE)
- Transition state theory (TST), 394  
Arrhenius equation for escape rate,  
396  
limit for, 397  
Maxwell–Boltzmann distribution,  
396
- TRPD, *see* Time-resolved  
photodissociation (TRPD)
- TST, *see* Transition state theory (TST)
- TTS, *see* Time-temperature  
superposition (TTS)
- Two-dimensional systems, for  
confined colloid suspensions,  
233–241  
adsorption as function of position,  
234  
2D phase transitions, 233–234  
equilibrium configurations, 235  
KTHNY theory, 237–241  
liquid-to-hexatic transition, 240  
magnetic dipole–dipole repulsion,  
237  
orientation correlation function,  
235  
percolation transition, 240  
q2D colloid suspension of hard  
squares, 236–237
- Two-dimensional systems, of  
confined colloid suspensions,  
233–241  
adsorption as function of position,  
234  
2D phase transitions, 233–234  
equilibrium configurations, 235

- KTHNY theory, 237–241
- liquid-to-hexatic transition, 240
- magnetic dipole–dipole repulsion, 237
- orientation correlation function, 235
- percolation transition, 240
- q2D colloid suspension of hard squares, 236–237
- Ultrafast dynamics and density matrix method, 366–383
  - Bixon–Jortner (B-J) model, 367–373
    - Hamiltonian with applied optical excitation, 370
    - Laplace transformation, 368–369
    - limitation of, 379–383
    - Liouville equation, 367
    - Markoff approximation, 369
    - optical absorption rate, 371
    - Pauli master equation, 369–370
    - polarization, 371–372
    - for probing, 379
    - for pumping, 371, 379
    - spectroscopies of
      - photosynthesis, 379–383
    - steady state approximation, 372
    - susceptibility, 372–373
  - general model, 373–383
    - first-order approximation, 374–375
    - perturbation method for
      - Lionville equation, 373–374
    - pumping effect of, 378
    - second-order approximation, 375–376
    - steady state approximation, 378–379
    - zeroth-order approximation, 374
  - overview, 366–367
  - ultrafast pulses, and von Neumann/Gabor theory, 11–14
- Very high damping (VHD), 398
- Very low damping (VLD) escape rate, 394–395, 399–401
  - assembly of particles in
    - double-well potential, 403
  - Boltzmann equilibrium and, 394
  - Brownian motion, 401–402
  - classical spins and, 441–446
    - for biaxial and uniaxial anisotropies, 446–449
  - first-order linear differential equation, 441
    - as flux-over-population, 442
    - longest relaxation time, 442, 447–448
    - magnetization reversal time, 446
    - normalized times versus barrier height parameter, 448, 449
    - reversal time for biaxial and uniaxial anisotropies, 446–449
  - saddle point energy, 443
  - steady state probability current, 441
    - Taylor series, 444
    - transformation matrix, 444
    - well angular frequency, 445
- connection with high frequency resonance absorption, 401–405
- connection with Mel'nikov's solution of Kramers turnover problem, 405–408
- critical energy curve, 400
- depopulation factor in, 407
- deterministic dynamics, 404
- double-well potential, 408
- dynamical approach, 395
- energy-controlled diffusion, 403
- energy distribution, 406
- energy-action diffusion equation, 406
- escape from single well, 404
- Fourier transforms, 406

- Very low damping (VLD) escape rate  
*(Continued)*  
 interwell relaxation, 401  
 multiplicative noise, 395  
 overall escape rate, 408  
 for particles with separable and  
 additive Hamiltonians,  
 419–421  
 first-order linear differential  
 equation, 419  
 MFPT approach, 420  
 over barrier, 421  
 rigid inertial rotator, 421  
 prefactor of, 404  
 separatrix in phase space, 399, 400  
 versus longest relaxation time  
 solutions, 421–424  
 Wiener–Hopf equation, 406–407  
 VHD, *see* Very high damping (VHD)
- Vibrational sum-frequency generation  
 (VSFG) spectroscopy, 296,  
 321–327  
 adiabatic approximation, 325–326  
 Condon approximation, 326  
 double-resonance, 324–325  
 IR and resonance Raman  
 scattering, 326  
 nonzero, 322  
 Placzek approximation, 321–322  
 von Neumann basis on infinite lattice,  
 5–6
- von Neumann/Gabor theory  
 applications to audio and image  
 processing, 28–31  
 applications to quantum mechanics,  
 14–28  
 and time-dependent Schrödinger  
 equation, 23–28  
 and time-independent  
 Schrödinger equation, 15–23  
 application to ultrafast pulses,  
 11–14  
 and biorthogonal von Neumann  
 basis set, 8–9  
 and FGH method, 20–21  
 and Fourier method, 6–7  
 on infinite lattice, 5–6  
 overview, 1–5  
 and periodic von Neumann basis,  
 7–8  
 with biorthogonal exchange,  
 9–11
- VSFG, *see* Vibrational SFG (VSFG)
- Wavelet generalization, and TISE,  
 21–23
- Yukawa interaction, 226–228
- Zero temperature phase diagram  
 in q1D systems, 232  
 in q2D systems, 250